CHEMICAL ENGINEERING TRANSACTIONS Volume 17, 2009
Editor Sauro Pierucci
 ISBN 978-88-95608-01-3 ISSN 1974-9791
DOI: 10.3303/CET0917087

On the dispersion of prolate ellipsoidal particles in turbulent channel flow

C. Marchioli[(1)], M. Fantoni[(1)] and Soldati A.[(1,2)]
[(1)] Dipartimento di Energetica e Macchine, Università degli Studi di Udine, via delle scienze 208, 33100, Udine (Italy)
[(2)]Centro Interdipartimentale di Fluidodinamica e Idraulica, Università degli Studi di Udine, via delle scienze 208, 33100, Udine (Italy)

In this paper, the dispersion of small prolate ellipsoidal particles in a directly simulated turbulent channel flow is investigated. Building on the results of previous studies (Zhang et al., 2001; Mortensen et al., 2008), we analyze the time evolution of particle orientation in an effort to clarify the influence of the particle aspect ratio, λ, and of the particle inertial response time, τ_p, on particle orientational behavior and, in turn, on particle preferential distribution and near-wall accumulation. Statistics obtained performing a parametric study in the (λ, τ_p)-space over a wide range of particle classes indicate that the preferred condition of streamwise alignment with the mean flow is unstable and can be maintained for rather short times before particles start to rotate around the spanwise axis. Results also indicate that the rotational motion of elongated particles affects the process of particle accumulation at the wall by changing from a quantitative viewpoint the deposition rates.

1. Introduction

Suspensions of tiny elongated particles in turbulent flows are commonly encountered in several industrial and environmental applications. Examples include aerosol and/or particulate dispersion in the atmosphere, pneumatic transport in pipes and channels, separation in cyclones and sediment transport in rivers. Previous experiments also show the ability of elongated fibers to reduce drag in fluid transport systems (Paschkewitz et al., 2005). Despite its practical importance, however, the problem of elongated particles dispersed in turbulent wall-bounded flows has become a topic for research only in recent years: among numerical Eulerian-Lagrangian works, the first Direct Numerical Simulation (DNS) of ellipsoidal particle transport and deposition in channel flow was performed by Zhang et al. (2001); followed by the complementary DNS of Mortensen et al. (2008). These studies showed that ellipsoidal particles, similarly to spherical particles, accumulate in the viscous sublayer and preferentially concentrate in regions of low-speed fluid velocity. Being "non isotropic", however, these elongated particles tend to align themselves with the mean flow direction, particularly very near the wall where their lateral tilting is suppressed.

Please cite this article as: Marchioli C., Fantoni M. and Soldati A., (2009), On the orientation of prolate ellipsoidal particles dispersed in turbulent channel flow, Chemical Engineering Transactions, 17, 519-524 DOI: 10.3303/CET0917087

In this paper, we investigate further on the problem by looking at the dynamical behavior of ellipsoidal particles, mimicking the dispersion of elongated rigid fibers, in a fully developed channel flow at moderate Reynolds number. The focus is on the combined influence of the particle aspect ratio and the particle response time on particle distribution, orientation, translation and rotation.

2. Problem Formulation and Governing Equations

The Eulerian fluid dynamics is governed by the continuity and Navier-Stokes equations written for incompressible, isothermal and Newtonian fluid. A pseudo-spectral flow solver is employed to solve such equations at a shear Reynolds number Re_τ=150, based on the shear velocity and the channel half height (corresponding to a bulk Reynolds number, Re=2250). The flow solver is based on the Fourier–Galerkin method in the streamwise (x) and spanwise (y) directions, whereas a Chebyshev-collocation method in the wall-normal direction (z). Time integration of fluid uses a second-order Adams–Bashforth scheme for the non-linear terms (which are calculated in a pseudo-spectral way with de-aliasing in the periodic directions) and an implicit Crank–Nicolson scheme for the viscous terms (Marchioli and Soldati, 2002).

The size of the computational domain is $4\pi h \times 2\pi h \times 2h$ in x, y and z, respectively; computations are carried out using $128 \times 128 \times 129$ grid points. Periodic boundary conditions are applied in x and y, no-slip conditions are enforced at both walls. The grid resolution is uniform in the homogeneous directions x and y, whereas a grid refinement (providing a minimum non-dimensional grid spacing of 0.045 wall units) is applied near the walls in the non-homogeneous direction, z. The non-dimensional step size for time integration is 0.045 in wall units.

Regarding the Lagrangian particle dynamics, the dispersed phase is treated in the same way as in Gallily and Cohen (1979), Zhang et al. (2001) and Mortensen et al. (2008). The translational equation of motion of an individual particle is given by the linear momentum equation: $d\boldsymbol{v}/dt=\boldsymbol{F}/m$, where $\boldsymbol{v}$ is the particle velocity, $\boldsymbol{F}$ is the total hydrodynamic drag force acting on the particle and $m=(4/3)\pi a^3\lambda\rho_p$ is the particle mass (a and λ are the semi-minor axis and the aspect ratio of the ellipsoid, whereas ρ_p is the density of the particle). The expression for $\boldsymbol{F}$ used in our simulations was first derived by Brenner (1963) for an ellipsoid under creeping flow conditions: $\boldsymbol{F}=\mu\boldsymbol{K}(\boldsymbol{u}-\boldsymbol{v})$, where μ is the fluid dynamic viscosity, $\boldsymbol{K}$ is the resistance tensor (whose components depend on the particle's orientation through the well-known Euler parameters) and $\boldsymbol{u}$ is the fluid velocity at particle position (obtained using a one-sided interpolation scheme based on sixth-order Lagrangian polynomials). The above particle equation of motion is advanced in time by means of a fourth-order Runge–Kutta scheme using the same step size as that of the fluid. The total tracking time in wall units was $t^+=1056$ (note that the superscript + is used in this paper to represent variables in non-dimensional form).

The relevant parameters to be specified for time integration are a, λ and the particle response time, $\tau_p^+=(2/9)(a^+)^2\, S\, f(\lambda)$, where S is the particle-to-fluid density ratio and $f(\lambda)$ is a logarithmic function of λ derived by Zhang et al. (2001). In this study, we have selected a^+=0.36, λ=1.001 (spherical particles), 3, 10, 50, and τ_p^+= 1, 5, 30, 100, thus extending the database of Mortensen et al. (2008) to 16 cases in the (λ, τ_p^+)-space. To

ensure converged statistics, swarms of N=200,000 particles are tracked for each particle category, assuming dilute flow conditions and one-way coupling between the phases.

3. Results and Discussion

Fig. 1 shows the instantaneous distribution of the $\tau_p^+ = 5$ particles with λ=50. Similar distributions are observed for the other particle categories, but they are not shown in this paper for sake of brevity. It is apparent that particles cluster into groups leaving regions empty of particles (Fig. 1a) and that particles are aligned with the mean flow direction. We remark here that the regions depleted of particles have the same location for all the particle categories investigated: this means that, regardless of the strong mathematical coupling between rotational and translational equations due to the dependency of the resistance tensor on the orientation, particle distributions are practically unaffected by the aspect ratio and depend only on the response time. This is also the case for many translational velocity statistics, as already observed by Mortensen et al. (2008). One important exception, however, is given by the particle wall-normal translational velocity, w_p'. Besides being strongly dependent on the particle response time, this quantity is also significantly influenced by λ as shown in Fig. 2 for the $\tau_p^+ = 5$ particles case (again, similar curves are obtained for the other particle categories, but they are not shown here for brevity). Note that the profiles in this figure were smoothed out by time-averaging over the last 200 wall time units of the simulation. Such time-averaging procedure was adopted for ease of comparison and for visualization purposes only: the

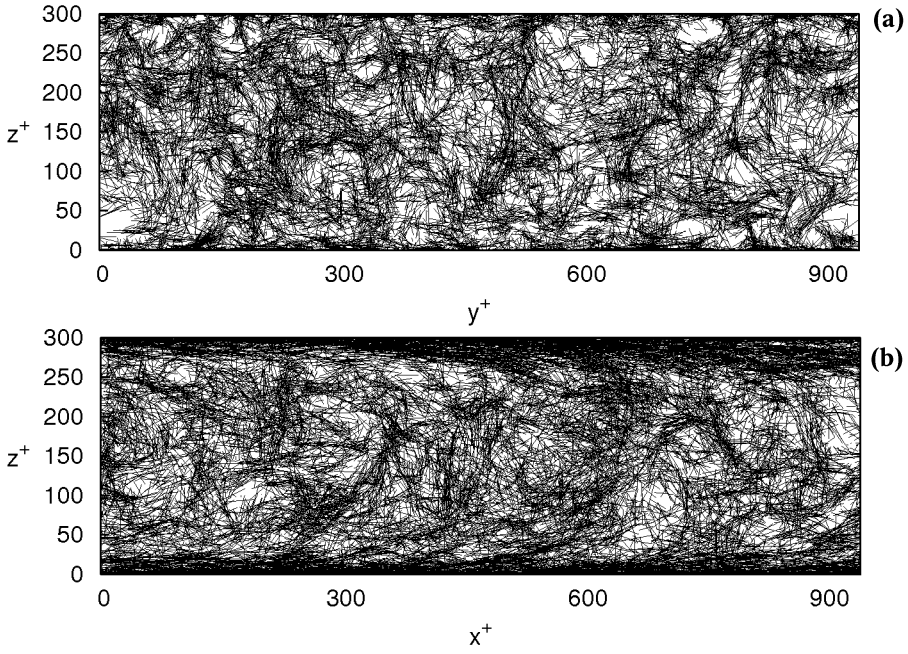

***Fig. 1**: Instantaneous particle distribution at the end of the simulation ($\tau_p^+ = 5$, λ=50). Panels: (a) cross-sectional view (mean flow directed towards the reader); (b) lateral view (mean flow directed from left to right).*

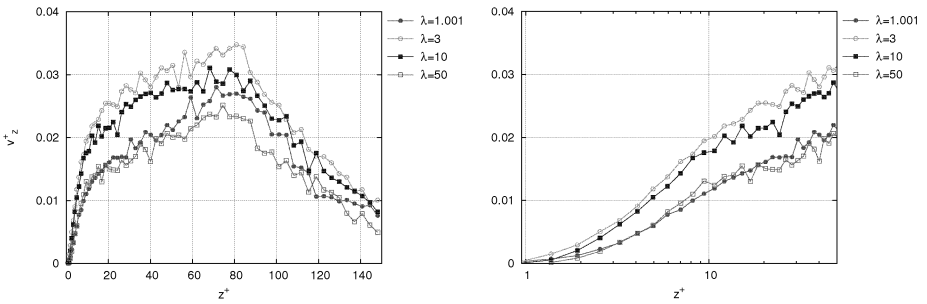

***Fig. 2**: Mean wall-normal translational velocity, w_p', for the τ_p^+= 5 particles. The right-hand panel shows a close-up view of the profiles in the near-wall region (log-lin plot).*

profiles considered refer to a statistically-developing condition for the particle concentration and, thus, w_p' is a time-dependent quantity which asymptotically tends to zero as the steady-state condition is approached. In the case shown, the aspect ratio produces a non monotonic variation of w_p' leading to a maximum increase for λ=3 and a subsequent decrease for λ=10 and λ=50. Conversely, for the larger τ_p^+=30 and τ_p^+=100 particles (not shown) we observe a monotonic decrease as λ increases.

This complex dependency of w_p' on both τ_p^+ and λ produces remarkable changes in the rate at which particles travel towards the wall and, in turn, modify the build-up of particles in the near-wall region, as shown by the instantaneous concentration profiles (computed as volumetric particle number density) of Fig. 3. From a quantitative viewpoint, the most evident changes occur in the very near-wall region (within a few wall units from the wall): each profile develops a peak of concentration which is located at different positions depending on the aspect ratio, and the peak value changes as well according to the variations of w_p' discussed above. Outside the viscous sublayer, variations are less evident and, again, the elongation of the particle does not seem to play an important role.

To investigate further the role of λ and τ_p, we analyzed the orientation statistics. In particular, we focused on the orientation time for each particle category. Here, we define the orientation time as the overall time spent by the particles in a given position of

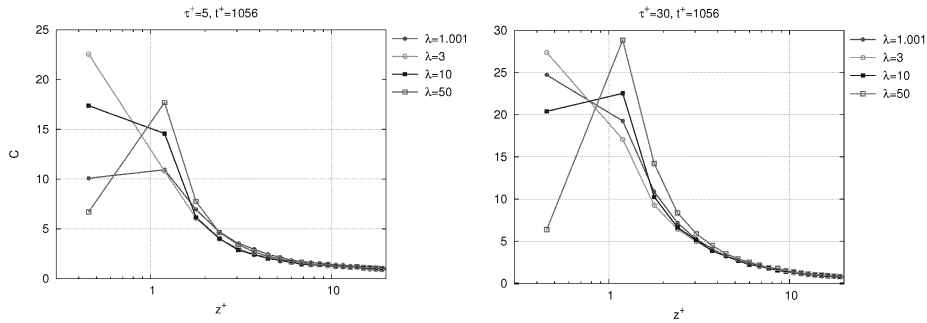

***Fig. 3:** Wall-normal particle concentration profiles. Left panel: τ_p^+=5 particles, right panel: τ_p^+=30 particles.*

alignment with respect to the mean flow. To perform this calculation, we proceeded for each particle category in the following way:

I) The alignment of each particle was classified by subdividing the absolute value of the direction cosines, $|\cos(\theta_i)|$, which determine the orientation of the particle with respect to the Cartesian axes, into 10 equally-spaced bins (e.g. 1st bin in the range [0,0.1], 2nd bin in the range [0.1,0.2], etc.). Particles are tagged as aligned with a given direction, x_i, if they fall in the bin where $|\cos(\theta i)|$ is in the range [0.9,1].

II) The orientation of each particle and the corresponding bin are obtained every time step over a long period of time ($T^+ = 200$ at the end of the simulation); a time-counter is then updated to compute the overall time, $t^+(i,j,k)$, spent by the i^{th} particle of the j^{th} category in the k^{th} bin.

III) The mean time per bin is computed as $t^+(j,k)=(1/N)\Sigma_i\ t^+(i,j,k)$ where $i=1,...,N$ and then its percentage value is obtained dividing by T^+.

Such procedure was applied focusing on two specific regions of the flow: a core region across the channel centerline ($140<z^+<160$) and a near-wall region ($z^+<10$ from the wall). In Fig. 4 we show the results obtained for $|\cos(\theta_x)|$ as a function of the different aspect ratios in the $\tau_p^+=5$ particles case. In the central regions of the channel (Fig. 4a) there is almost no mean shear and turbulence is nearly homogeneous and isotropic so that no preferential particle is observed. More interesting observations can be made in the near-wall region: even though, as demonstrated by Zhang et al. (2001) and by Mortensen et al. (2008), the most probable particle orientation is in the streamwise direction, Fig. 4b indicates that particles are aligned with the mean flow at most 50% of the time in the most favorable case (λ=50), whereas the percentage orientation time falls to about 30% for λ=3. For the $\tau_p^+=30$ particles case (not shown) the percentage orientation time is slightly below 30%, irrespectively of the aspect ratio. Considering also the results for the spanwise and wall-normal direction cosines (not shown), we can conclude that the position of near-wall alignment imposed by the streamwise fluctuations of the flow, though statistically probable, is quite "unstable". In other words, it can not be maintained for very long times before the wall-normal fluid velocity gradient induces a nearly planar rotation of the initially-aligned particles around the spanwise direction.

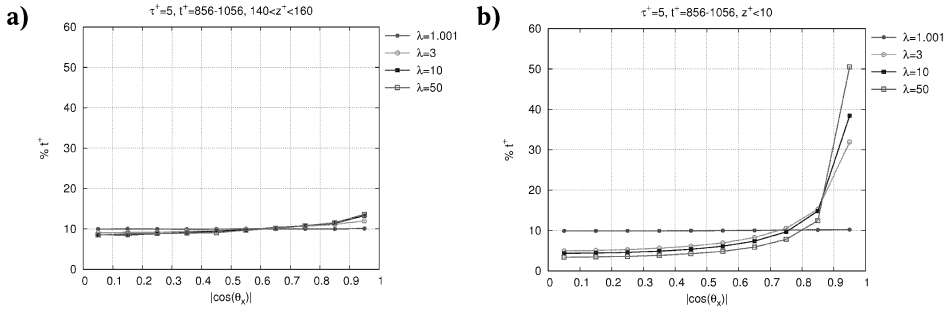

***Fig. 4**: Streamwise orientation time (% values) for the $\tau_p^+=5$ particles. Panels: (a) channel center; (b) near-wall region.*

Such observables are important to interpret, from a physical viewpoint, the combined effect of particle shape and inertia on macroscopic phenomena like particle wall accumulation and particle segregation, which depend on the nature of particle dynamics in connection with turbulence dynamics (Marchioli and Soldati, 2002). Note that, since the direction cosines are non-linear functions, equally-spaced bins for $|\cos(\theta_i)|$ correspond to bins of different "size" for θ_i, the "alignment" bin being wider than the others. We thus expect that new results computed considering equally-spaced bins for θ_i would lead to the same (probably even more striking) qualitative conclusion.

4. Conclusions

In the present work, the dynamics of prolate ellipsoidal particles dispersed in a turbulent channel flow was analyzed using DNS and Lagrangian particle tracking. Prolate ellipsoids were chosen because they reproduce quite reasonably the behavior of rigid fibers in a number of applications of both scientific and engineering interest.

Results obtained for several combination of values sampling the (λ, τ_p)-space indicate clearly that the rotational motion of elongated particles affects the turbulence-induced net flux of particles toward the wall by changing the mean particle wall-normal velocity. This effect, which can ultimately be ascribed to the shape of the particles, adds to that due to their inertia and, compared to the case of spherical particles, modifies from a quantitative viewpoint the build-up of particles at the wall and the deposition rates, as demonstrated by the concentration profiles. One possible explanation for such observable can be found by looking at particle rotational dynamics: as shown by the analysis of the near-wall particle orientation times, the preferred condition of streamwise alignment with the mean flow is unstable and can be maintained for rather short times before particles are forced to rotate around the spanwise axis by the shear-induced wall-normal velocity gradient, thus changing their local spatial distribution.

The main future development of this work is the inclusion of two-way coupling effects in the simulations. Hopefully, through these new simulations it will be possible to provide a physical explanation to the mechanism of fiber-induced turbulent drag reduction, which has been observed in many experiments.

References

Brenner H., 1963, The Stokes resistance of an arbitrary particle, Chem. Eng. Sci., 18, 1-25.

Gallily I. and Cohen A., 1978, On the orderly nature of the motion of nonspherical aerosol particles, J. Colloid Interf. Sci., 68, 338-356.

Marchioli C. and Soldati A., 2002, Mechanism for particle transfer and segregation in turbulent boundary layer, J. Fluid Mech., 468, 283-315.

Mortensen P.H., Andersson H.I., Gillissen J.J.J., and Boersma B.J., 2008, Dynamics of prolate ellipsoidal particles in a turbulent channel flow, Phys. Fluids, 20, 093302.

Paschkewitz J.S., Dubief Y., and Shaqfeh E.S.G., 2005, An experimental and numerical investigation of drag reduction in a turbulent boundary layer using a rigid rodlike polymer, Phys. Fluids, 17, 085101.

Zhang H., Ahmadi G., Fan F.G., and McLaughlin J.B., 2001, Ellipsoidal particles transport and deposition in turbulent channel flows, Int. J. Multiphase Flow, 27, 971-1009.